Nonlinear Disturbance Decoupling for a Mobile Robotic Manipulator over Uneven Terrain

Joel Jimenez-Lozano * **Bill Goodwine** **

* *Department of Aerospace and Mechanical Engineering, University of Notre Dame, Notre Dame, IN 46556, USA (e-mail: jjimene1@nd.edu)*
** *Department of Aerospace and Mechanical Engineering, University of Notre Dame, Notre Dame, IN 46556, USA (e-mail: billgoodwine@nd.edu)*

Abstract: This paper considers the nonlinear disturbance decoupling problem for a robotic manipulator that is mounted on a mobile platform. A mobile manipulation system offers a dual advantage of mobility offered by a mobile platform and dexterity offered by the manipulator. In this work, the tracking and nonlinear disturbance decoupling problems are studied with particular focus on disturbances due to uneven terrain. We show that this system possesses the necessary geometric structure for complete disturbance decoupling between the outputs and disturbances. The disturbances are modeled as changes in the effect of gravitational forces on the mobile manipulator due to its motion over a uneven terrain. Simulation results illustrate complete disturbance decoupling even in the presence of significant disturbances using the designed nonlinear controller.

1. INTRODUCTION

This paper presents results for complete nonlinear disturbance decoupling for a manipulator mounted on a mobile platform subjected to varying gravitational forces due to uneven terrain. A mobile manipulators built from a robotic arm mounted on a wheeled mobile platform provides better capabilities for numerous tasks. A mobile manipulator combines the dexterous manipulation capability offered by the manipulator and the motility provided by the mobile platform. Investigation of their stability, control design, simulation and experimentation for different situations has been studied by many researchers including Chen and Zalzala [1997], Wang and Kumar [1993], Chung and Velinsky [1998], Nikoobin and Rahimi [2009] and others.

Yamamoto and Yun [1996] studied the effect of the dynamic interaction between the manipulator and the mobile platform and showed that the system was feedback linearizable under the appropriate nonlinear change of coordinates. The manipulator tracks a desired trajectory in a fixed reference frame. Their objective was to compensate the dynamic interaction through a nonlinear feedback to improve the performance of the overall system. A modular approach of this analysis was presented in Yamamoto and Yun [1997] which includes a detailed proof of the functional dependence of some of the dynamic terms of the equations. In this work, that methodology will be extended in studying a mobile manipulator in which we will include external force disturbances into the system. The final goal of the disturbance decoupling problem is to find a state feedback law such that the output is unaffected by the disturbance. Related work on disturbance decoupling have been studied on robotic manipulators and mobile platforms in Nijmeijer [1983], Danesh et al. [2005], Joshi and Desrochers [1986], Zhu et al. [1993], Gao [2006], Papadopoulos and Paraskevopoulos [1985], Estrada and Malabre [2002] and others.

In the following sections, we present the dynamic equations of the mobile manipulator which are coupled. A state space representation of the equations is presented which extends the derivation in Yamamoto and Yun [1996]. A nonlinear feedback controller is designed, which includes disturbance decoupling. The calculation of disturbance forces due to the motion of the mobile platform over an uneven terrain is presented and simulation results are presented which illustrate the position of the mobile manipulator during motion to follow individual task trajectories for the platform and arm, and other variables. It is shown that the outputs are completely decoupled from the disturbances. The main contribution of this paper is applying the disturbance decoupling method to a problem with practical utility and with a level of complexity similar to real-world problems.

2. MODELING EQUATIONS

The equation of motion of the *robotic manipulator* subject to vehicle motion Yamamoto and Yun [1996, 1997] can be extended to include external force disturbances, and it is given by

$$M_r(q_r)\ddot{q}_r + C_{r1}(q_r, \dot{q}_r) + C_{r2}(q_r, \dot{q}_r, q_v)$$
$$= \tau_r - R_r(q_r, q_v)\ddot{q}_v + J_{r1}{}^T(q_r)F_e{}^{r1} + J_{r2}{}^T(q_r)F_e{}^{r2}, \quad (1)$$

where $q_r = [\theta_1, \theta_2]^T$ denotes the Lagrangian coordinates of a 2R manipulator, q_v denotes the Lagrangian coordinates of the mobile platform, M_r is the inertia Matrix, C_{r1} represents the Coriolis and centrifugal terms, C_{r2} denotes the Coriolis and

centrifugal terms caused by the angular motion of the platform, τ_r is the input torque/force for the manipulator, R_r is the inertia matrix which represents the effect of the vehicle dynamics on the manipulator, F_e^{r1} and F_e^{r2} are external force disturbance vectors on the center of gravity on each arm link and $J_{r1}^T(q_r)$ and $J_{r2}^T(q_r)$ is the task space Jacobian matrix of each arm link. Each term matrix/vector is presented in the Appendix.

The equation of motion of the *mobile platform* with a mounted manipulator Yamamoto and Yun [1996, 1997] including external force disturbances is given by

$$M_{v1}(q_v)\ddot{q}_v + C_{v1}(q_v,\dot{q}_v) + C_{v2}(q_r,\dot{q}_r,q_v,\dot{q}_v) = E_v\tau_v - A^T\lambda$$
$$- M_{v2}(q_r,q_v)\ddot{q}_v - R_v(q_r,q_v)\ddot{q}_r + E_vJ_v^T(q_v)F_e^v, \quad (2)$$

where q_v denotes the Lagrangian coordinates of the mobile platform and will be described in the next section, M_{v1} and C_{v1} are the mass inertia and the velocity dependent terms of the platform, respectively, M_{v2} and C_{v2} represent the inertial term and Coriolis and centrifugal terms due to the presence of the manipulator, τ_v is the input torque/force to the vehicle, E_v is a constant matrix, λ denotes the vector Lagrange multipliers corresponding to the kinematic constraints, R_v represents the inertia matrix which reflects the dynamic effect of the arm motion on the vehicle, F_e^v is an external force disturbance vector on the mobile platform through its center and $J_v^T(q_v)$ is the moving space Jacobian matrix for the mobile platform. Combining the velocity and inertia terms in Eqn. (1) and Eqn. (2), respectively, equations of motion of the wheeled mobile manipulator are simplified to

$$M_r(q_r)\ddot{q}_r + C_r(q_r,\dot{q}_r,\dot{q}_v) = \tau_r - R_r(q_r,q_v)\ddot{q}_v$$
$$+ J_{r1}^T(q_r)F_e^{r1} + J_{r2}^T(q_r)F_e^{r2}$$
$$M_v(q_r,q_v)\ddot{q}_v + C_v(q_r,q_v,\dot{q}_r,\dot{q}_v) = E_v\tau_v \quad (3)$$
$$- R_v(q_r,q_v)\ddot{q}_r - A^T\lambda + E_vJ_v^T(q_v)F_e^v,$$

where $C_r = C_{r1} + C_{r2}$, $C_v = C_{v1} + C_{v2}$ and $M_v = M_{v1} + M_{v2}$.

2.1 Constraint Equations of the Mobile Platform

The following notation will be used in the derivation of the constraint and dynamic equations, as is illustrated in Fig. 1.

(1) For the mobile platform, (x_0, y_0) are the coordinates of the point P_0 which is the intersection of the axis of symmetry with the driving wheel axis in the inertial frame, b is the distance between the driving wheels and the axis of symmetry, r is the radius of each driving wheel, θ_r and θ_l are the angular positions of the right and left driving wheel, respectively, $\phi = r(\theta_r - \theta_l)/2b = c(\theta_r - \theta_l)$ is the heading angle of the mobile robot measured from ^wX-axis, d is the distance from P_0 to the center of mass of the platform, m_c is the mass of the platform without the driving wheels and I_c is the moment of inertia of the platform without the driving wheels about a vertical axis through P_0.
(2) For the manipulator, $P_b = (^vx_b, ^vy_b)$ are the coordinates of the base of the manipulator in the frame Σ_v, θ_1 and θ_2 are the joint angles of the manipulator, l_1 and l_2 are the arm lengths, respectively, m_w is the mass of each driving wheel and I_m is the moment of inertia of each wheel and the motor about the wheel diameter.

The mobile platform has two co-axial wheels driven by motors. There are three constraints to which the platform is subjected, one is that the platform must move in the direction of the axis of
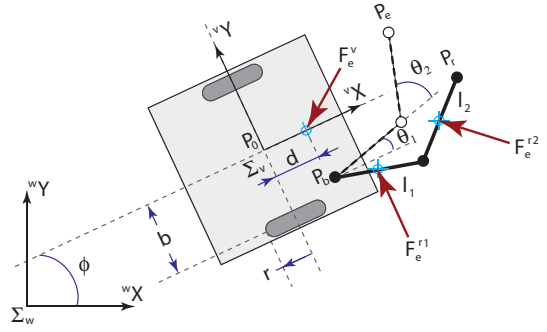

Fig. 1. Geometry of the mobile platform and the mounted 2R manipulator.

symmetry, and the other two are rolling constraints, i.e. driving wheels do not slip. The constraint equations are given in matrix form as $A(q_v)\dot{q}_v = 0$, where $q_v = [x_0, y_0, \theta_r, \theta_l]^T$ and $A(q_v)$ is given by

$$A(q_v) = \begin{bmatrix} -\sin\phi & \cos\phi & 0 & 0 \\ -\cos\phi & -\sin\phi & cb & cb \end{bmatrix}. \quad (4)$$

2.2 State Space Formulation of Motion Equations

The dynamics of the wheeled mobile manipulator are governed by Eqns. (3) and $A(q_v)\dot{q}_v = 0$. Since the platform velocity is always in the null space of $A(q_v)$ Yamamoto and Yun [1996], from $A(q_v)\dot{q}_v = 0$, it is possible to define a vector of generalized coordinates $\eta(t)$ such that $\dot{q}_v = S(q_v)\eta(t)$, where $S(q_v)$ is a 4×2 full rank matrix, whose columns are in the null space of $A(q_v)$. Thus

$$S(q_v) = \begin{bmatrix} cb\cos\phi & cb\cos\phi \\ cb\sin\phi & cb\sin\phi \\ 1 & 0 \\ 0 & 1 \end{bmatrix}.$$

Differentiating $\dot{q}_v$, substituting for $\ddot{q}_v$ into the first equation in Eqns. (3) and multiply by S^T. Following a similar procedure for $\ddot{q}_v$, which is substituted into the second equation in Eqns. (3) results in the system of equations

$$\underbrace{\begin{bmatrix} S^T M_v S & S^T R_v \\ R_r S & M_r \end{bmatrix}}_{P} \begin{bmatrix} \dot{\eta} \\ \ddot{q}_r \end{bmatrix} =$$

$$\underbrace{\begin{bmatrix} -S^T M_v \dot{S}\eta - S^T C_v \\ -C_r - R_r\dot{S}\eta \end{bmatrix}}_{\xi} + \underbrace{\begin{bmatrix} S^T E_v & 0 \\ 0 & I \end{bmatrix}}_{Q} \begin{bmatrix} \tau_v \\ \tau_r \end{bmatrix}$$

$$+ \underbrace{\begin{bmatrix} S^T E_v J_v^T & 0 \\ 0 & 0 \end{bmatrix}}_{D_1} \begin{bmatrix} F_e^v \\ 0 \end{bmatrix} + \underbrace{\begin{bmatrix} 0 & 0 \\ 0 & J_{r1}^T \end{bmatrix}}_{D_2} \begin{bmatrix} 0 \\ F_e^{r1} \end{bmatrix}$$

$$+ \underbrace{\begin{bmatrix} 0 & 0 \\ 0 & J_{r2}^T \end{bmatrix}}_{D_3} \begin{bmatrix} 0 \\ F_e^{r2} \end{bmatrix}.$$

Using the state vector $x = [q_v^T \ q_r^T \ \eta^T \ \dot{q}_r^T]^T$, the system can be rewritten as

$$\dot{x} = \underbrace{\begin{bmatrix} S\eta \\ \dot{q}_r \\ P^{-1}\xi \end{bmatrix}}_{F(x)} + \underbrace{\begin{bmatrix} 0 \\ 0 \\ P^{-1}Q \end{bmatrix}}_{G(x)} \tau + \underbrace{\begin{bmatrix} 0 \\ 0 \\ P^{-1}D_1 \end{bmatrix}}_{p_1(x)} \omega_1$$

$$+ \underbrace{\begin{bmatrix} 0 \\ 0 \\ P^{-1}D_2 \end{bmatrix}}_{p_2(x)} \omega_2 + \underbrace{\begin{bmatrix} 0 \\ 0 \\ P^{-1}D_3 \end{bmatrix}}_{p_3(x)} \omega_3,$$

where $\tau = [\tau_v \ \tau_r]^T$, $\omega_1 = [F_e{}^v \ 0]^T$, and $\omega_2 = [0 \ F_e{}^{r1}]^T$ and $\omega_3 = [0 \ F_e{}^{r2}]^T$. Hence, the state space form is

$$\dot{x} = F(x) + G(x)\tau + p_1(x)\omega_1 + p_2(x)\omega_2 + p_3(x)\omega_3. \quad (5)$$

3. FEEDBACK CONTROL AND DISTURBANCE DECOUPLING

In this section, subsection 3.1 derives the output equations and follows Yamamoto and Yun [1996]. Subsection 3.2 includes disturbance decoupling results not presented in their work.

3.1 Output Equations

The desired task trajectory for the endpoint of the manipulator P_e in the frame Σ_w is given by

$$^w P_e(t) = \begin{bmatrix} ^w x_e(t) \\ ^w y_e(t) \end{bmatrix}.$$

The mobile manipulator shown in Fig. 1 has four inputs, two from the 2R manipulator and two from the mobile platform. We may have up to four output variables to be controlled. First, we select the output variables of the manipulator to be P_e, which represents the actual location of the end point of the manipulator. The coordinates of P_e with respect to the platform coordinate frame Σ_v are given by

$$^v P_e = \begin{bmatrix} ^v x_e \\ ^v y_e \end{bmatrix} = \begin{bmatrix} l_1 \cos\theta_1 + l_2 \cos(\theta_1 + \theta_2) + {}^v x_b \\ l_1 \sin\theta_1 + l_2 \sin(\theta_1 + \theta_2) + {}^v y_b \end{bmatrix},$$

where the points $^v P_e$ and $^w P_e$ are related by

$$^w P_e = {}^w P_0 + R_\phi {}^v P_e = \begin{bmatrix} x_0 \\ y_0 \end{bmatrix} + \begin{bmatrix} \cos\phi & -\sin\phi \\ \sin\phi & \cos\phi \end{bmatrix} \begin{bmatrix} ^v x_e \\ ^v y_e \end{bmatrix}.$$

The output variables for controlling the mobile platform are chosen next. The objective of the platform movement is to bring the manipulator into a preferred configuration. For this purpose, we pick the configuration with the maximum manipulability measure as the preferred configuration of the manipulator. The manipulability measure can be regarded as a distance measure of the manipulator configuration from singular ones at which the manipulability becomes zero. At or near a singular configuration, the endpoint of the manipulator may not easily move in certain directions. The effort of maximizing manipulability measure leads to keeping the manipulator configuration away from singularity. The manipulability measure for nonredundant manipulators $w = l_1 l_2 |\sin\theta_2|$ Yoshikawa [1990], and is maximized for $\theta_2 = \pi/2$ and arbitrary θ_1. The endpoint of the manipulator at the preferred configuration is denoted by P_r, called the reference point. The coordinates of P_r in Σ_v are given by

$$^v P_r = \begin{bmatrix} ^v x_r \\ ^v y_r \end{bmatrix} = \begin{bmatrix} \sqrt{l_1{}^2 + l_2{}^2} + {}^v x_b \\ ^v y_b \end{bmatrix} = \begin{bmatrix} l_x \\ l_y \end{bmatrix}.$$

We look to control the mobile platform in such a way that P_r is brought to P_e, so the manipulator is brought into the preferred configuration. Thus, we select the coordinates of P_r in the inertial frame Σ_w, i.e.,

$$^w P_r = \begin{bmatrix} ^w x_r \\ ^w y_r \end{bmatrix} = \begin{bmatrix} x_0 \\ y_0 \end{bmatrix} + \begin{bmatrix} \cos\phi & -\sin\phi \\ \sin\phi & \cos\phi \end{bmatrix} \begin{bmatrix} l_x \\ l_y \end{bmatrix}$$

to be the other two components of the output equation. The output equations for controlling the mobile manipulator are given by

$$y = \underbrace{\begin{bmatrix} ^w x_r(x_0, y_0, \theta_r, \theta_l) \\ ^w y_r(x_0, y_0, \theta_r, \theta_l) \\ ^v x_e(\theta_1, \theta_2) \\ ^v y_e(\theta_1, \theta_2) \end{bmatrix}}_{h(x)}. \quad (6)$$

The objective of selecting these outputs is that the system is nonholonomic and it is not input state linearizable, it is input-output linearizable if a proper set of output equations are chosen. In addition, these set of outputs made the system proper for disturbance decoupling as shown next.

3.2 Feedback Input-Output Linearization with Disturbance Decoupling

We have presented the dynamics of the mobile manipulator in the state space form Eqn. (5) and the output equation Eqn. (6). The vector field is modeled through the $p(x)$s. To achieve input-output linearization a nonlinear feedback has to be employed. To simplify state Eqn. (5) we applied the following feedback,

$$\tau = Q^{-1}(Pu - \xi), \quad (7)$$

which simplifies the state equation as

$$\dot{x} = \underbrace{\begin{bmatrix} S\eta \\ \dot{q}_r \\ 0 \end{bmatrix}}_{f(x)} + \underbrace{\begin{bmatrix} 0 \\ 0 \\ I \end{bmatrix}}_{g} u + \underbrace{\begin{bmatrix} 0 \\ 0 \\ P^{-1}D_1 \end{bmatrix}}_{p_1(x)} \omega_1$$

$$+ \underbrace{\begin{bmatrix} 0 \\ 0 \\ P^{-1}D_2 \end{bmatrix}}_{p_2(x)} \omega_2 + \underbrace{\begin{bmatrix} 0 \\ 0 \\ P^{-1}D_3 \end{bmatrix}}_{p_3(x)} \omega_3, \quad (8)$$

$$y = h(x).$$

If the disturbances ω, are available for measurements one can use a control $u = \alpha(x) + \beta(x)v + \gamma_1(x)\omega_1 + \gamma_2(x)\omega_2 + \gamma_3(x)\omega_3$ Isidori [2002]. Then decoupling the output from the disturbance it is possible. The relative degree of the system is $r = 2$, that is the number of differentiations of each component of the outputs until the input explicitly appears in the derivative $\ddot{y}$. Following the analysis of Isidori [2002], the control law solving the problem of decoupling y is given by

$$\alpha(x) = -\frac{L_f^2 h(x)}{L_g L_f h(x)} = -\frac{\dot{\Phi}}{\Phi}\begin{bmatrix}\eta\\\dot{q}_r\end{bmatrix},$$

$$\beta(x) = \frac{1}{L_g L_f h(x)} = \frac{1}{\Phi},$$

$$\gamma_1(x) = -\frac{L_{p_1} L_f h(x)}{L_g L_f h(x)} = -P^{-1} D_1,$$

$$\gamma_2(x) = -\frac{L_{p_2} L_f h(x)}{L_g L_f h(x)} = -P^{-1} D_2,$$

$$\gamma_3(x) = -\frac{L_{p_3} L_f h(x)}{L_g L_f h(x)} = -P^{-1} D_3.$$

So, the nonlinear feedback is given by

$$u = \Phi^{-1}\left(v - \dot{\Phi}\begin{bmatrix}\eta\\\dot{q}_r\end{bmatrix} - \Phi P^{-1}(D_1\omega_1 + D_2\omega_2 + D_3\omega_3)\right). \quad (9)$$

The matrix Φ is presented in the Appendix. Substituting this nonlinear feedback Eqn. (9) into Eqn. (8), we obtain a linear and decoupled input-output relationship

$$\ddot{y} = \begin{bmatrix}\ddot{y}_1\\\ddot{y}_2\\\ddot{y}_3\\\ddot{y}_4\end{bmatrix} = \begin{bmatrix}v_1\\v_2\\v_3\\v_4\end{bmatrix} = v.$$

The input-output relationship is decoupled because each component of the reference input, v_i, controls one and only one component of the output y_i. To complete the controller design, it is necessary to stabilize each of the above four subsystem with another constant feedback. Therefore, the entire controller for the mobile manipulator consists of nonlinear feedback Eqn. (7) and Eqn. (9), followed by a linear feedback. We have used a PD computed-torque control law. We look for a desired trajectory y_d, which gives $\ddot{y} = \ddot{y}_d - K_v\dot{e} - K_p e$ with the tracking error defined as $e = y - y_d$. For our simulations, $K_v = 15$ and $K_p = 56$ were selected. Our algorithm requires the calculation of matrix operations, i.e. matrix inverse. During the simulation we tracked the condition number of the matrices in order to maintain stability. We used values of K_v and K_p that are well behaved and asymptotically decay to a constant value once the tracking errors are diminished.

4. DISTURBANCE FORCES

We are interested in disturbance forces that are position dependent. In this case, we have assumed that the disturbances are related to changes in the gravitational forces on the system due to the motion of the mobile manipulator over a uneven terrain. The uneven terrain is modeled as a surface function $U(x,y)$. The surface must be known or the robot must be equipped with a sensor that can determine the orientation of the gravity vector. The form of the terrain for the simulations in this paper is illustrated in Fig. 3 and the trajectory used for the simulations projected onto the x-y plane is indicated by the solid line. For clarity of presentation, the robot is modeled as moving along a flat surface, but subjected to a force field that would result from the uneven terrain.

A unit normal can be calculated at each point on the surface (or sensed if the robot is there) using $n = \nabla U / \|\nabla U\| = n_x\hat{i} + n_y\hat{j} + n_z\hat{k}$. This normal vector is used to project the force due to gravity onto the XY-plane. The gravitational forces are given by $W_{cart} = -m_w g\hat{k}$ for the cart, $W_{link1} = -m_1 g\hat{k}$ and $W_{link2} = -m_2 g\hat{k}$ for each link, respectively. The forces are obtained by using

$$F_e{}^v = \left(\frac{n \cdot W_{cart}}{\|n\|^2}\right)n, \quad (10)$$

$$F_e{}^{r1} = \left(\frac{n \cdot W_{link1}}{\|n\|^2}\right)n, \quad (11)$$

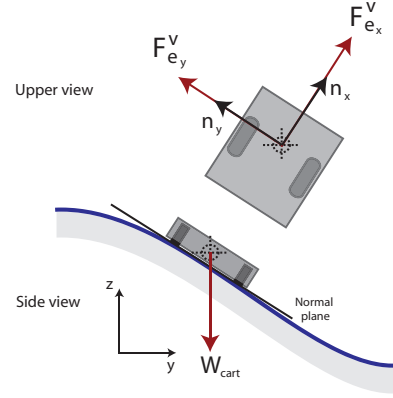$$F_e{}^{r2} = \left(\frac{n \cdot W_{link2}}{\|n\|^2}\right)n. \quad (12)$$
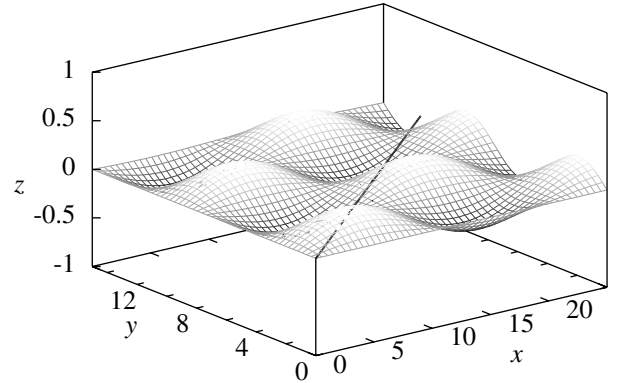

Fig. 2. Modeling of the disturbance forces.

Fig. 3. Disturbance forces on the mobile platform and the uneven terrain. Surface function $U = 0.25\sin(0.5x)\sin(0.5y)$.

5. SIMULATIONS

This section presents simulation results illustrating the effectiveness of the controller. In the simulation, individual task trajectories for the mobile platform and arm are investigated. The mobile platform is initially placed at the origin facing toward the positive ${}^wX$-axis of the inertial frame. The initial head angle is zero, $\phi(0) = 0$. Platform and manipulator parameter values are given in Table 1, we have used the values used in Yamamoto and Yun [1996]. The entire system is assumed to be stationary at $t = 0$. The initial values are $(x_0, y_0, \theta_r, \theta_l, \theta_1, \theta_2, \dot{\theta}_r, \dot{\theta}_l, \dot{\theta}_1, \dot{\theta}_2) = (-0.25, -0.25, 0, 0, 70,$

Table 1. Parameters values used for the simulation

Parameters	Values	Units
r	0.075	m
b	0.171	m
l_1	0.4	m
l_2	0.4	m
m_1	4	kg
m_2	4	kg
m_c	94	kg
m_w	5	kg
I_c	6.609	$kg \cdot m^2$
I_m	0.135	$kg \cdot m^2$
I_w	0.010	$kg \cdot m^2$
d	0	m

$-70, 0, 0, 0, 0)$. Individual task trajectories for mobile platform and arm are

$$
{}^w P_e(t) = \begin{bmatrix} {}^w x_r(t) \\ {}^w y_r(t) \\ {}^v x_e(t) \\ {}^v y_e(t) \end{bmatrix} = \begin{bmatrix} {}^v x_e(0) + \dfrac{3}{10}t \\ {}^v y_e(0) + \dfrac{3}{20}t \\ {}^m x_e(0) \\ {}^m y_e(0) + 0.7 \sin\left(\dfrac{\pi}{4}t\right) \end{bmatrix},
$$

where $({}^v x_e(0), {}^v y_e(0)) = (0,0)$ and $({}^m x_e(0), {}^m y_e(0)) = (-0.1, -0.1)$. The location of the arm base on the mobile platform are given by ${}^v x_b = 0.01 \mathrm{m}$ and ${}^v y_b = -0.01 \mathrm{m}$.

The cart geometry and its center $(+)$ are shown in Fig. 4, the straight solid line represents the mobile platform trajectory and the sinusoidal solid line represents the trajectory of the end-point of the manipulator. Platform and arm positions are shown at different times, the total period of time for the simulation was 90 seconds. The variations of the joint angles of the manipulator during time are shown in Fig. 5. The variation of the heading angle of the platform during the simulation is shown in Fig. 6. The tracking errors are shown in Fig. 7. We have estimated the tracking error as the difference of the obtained trajectory to the desired trajectory as $e_i(t) = y_i(t) - y_{d_i}(t)$, for $i = 1, \ldots, 4$. Initially there are oscillations in the tracking error, but later are reduced to very low values as expected.

The outputs are completely decoupled from the disturbance forces; hence, the outputs do not change with the disturbances. The effect of force disturbance can be observed in the torques required during the motion of the system. The disturbance forces has been implemented assuming a surface $U = 0.25 \sin(0.5x) \cos(0.5y)$ and forces were calculated using the methodology discussed in Section 4. The disturbance force components on the mobile platform during time are shown in Fig. 8. The computed torques for control are shown in Fig. 9.

The disturbance force components on the arm links are shown in Fig. 10. The computed torques for control are shown in Fig. 11. It can be observed that the disturbances are satisfactorily managed by the linear control applied to the linear input-output relationship.

6. CONCLUSIONS

We have presented the solution to the disturbance decoupling problem for a system with a manipulator mounted on a mobile
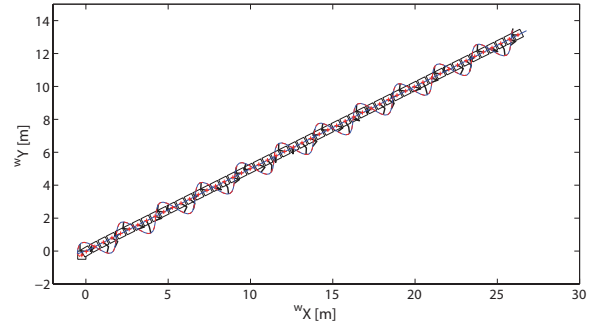
(a) Simulation
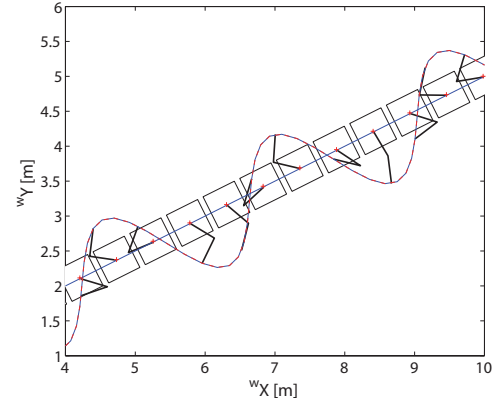
(b) Close-up view

Fig. 4. Motion of the mobile platform and arm during individual task trajectories. Solid straight line, linear task trajectory; Solid sinusoidal line, tip of the arm; $+$, P_0; dashed square; mobile platform position.
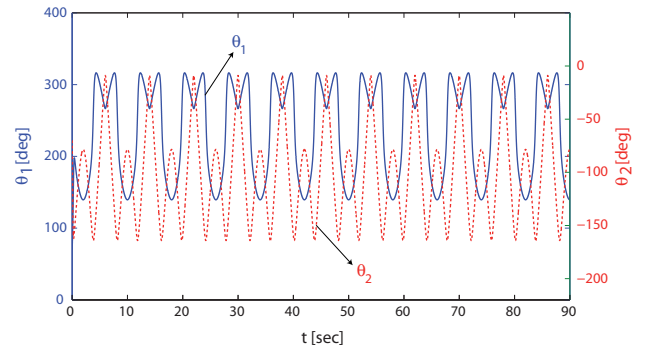

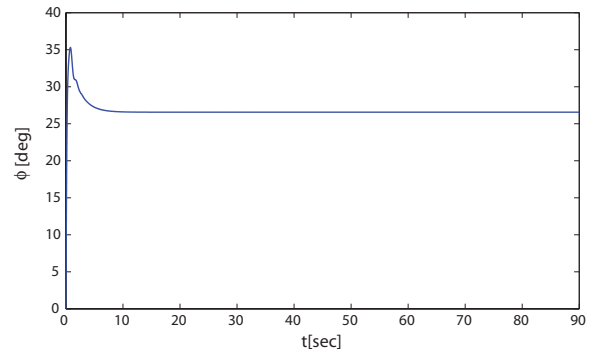Fig. 5. Joint angles of the manipulator in time.

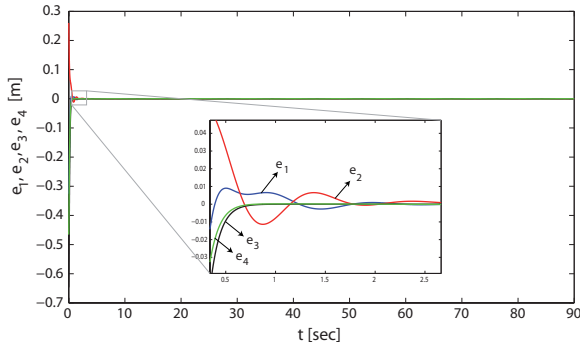Fig. 6. Heading angle of the mobile platform in time.
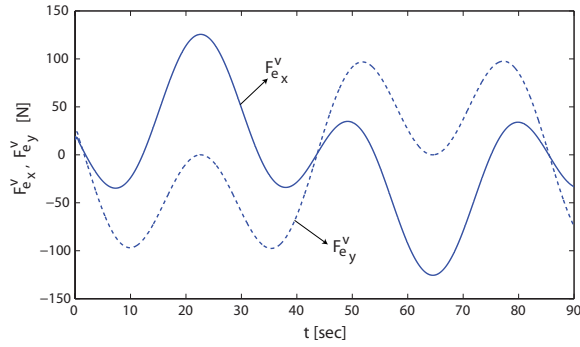
Fig. 7. Tracking errors.

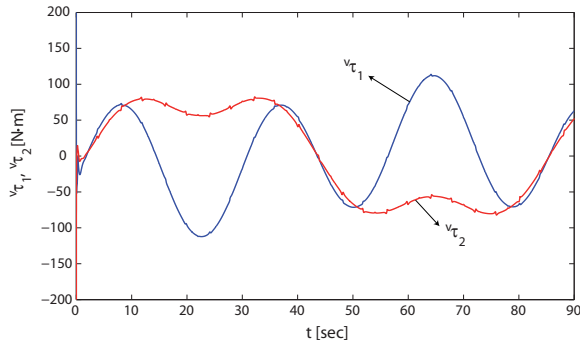Fig. 8. Disturbance forces on the platform.

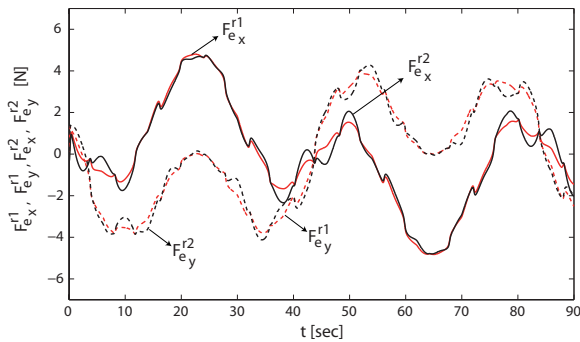Fig. 9. Computed platform torques for the platform.

Fig. 10. Disturbance forces on the arm links.

platform. The efficacy of the approach is illustrated by imposing a force field on the system that would result from the mobile platform traversing uneven terrain. Future work will involve incorporating recent results of the authors related to the control of mechanical systems and the notion of dynamic singularities Goodwine and Nightingale [2010] in order to extend these results to more complicated systems. Also, a experimental study
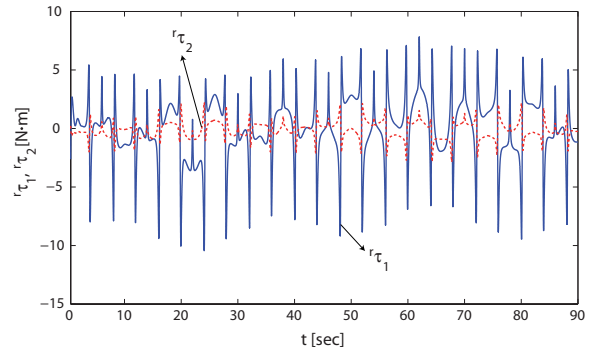

Fig. 11. Computed arm joint torques.

on a real mobile manipulator system will be made to implement our algorithm and enforce our results.

REFERENCES

D. P. Papadopoulos and P. N. Paraskevopoulos. Decoupling Techniques applied to the design of a controller for an unregulated synchronous machine. *General, Transmission and Distribution, IEE Proceedings C*, 132(6):277–280, 1985.

H. Nijmeijer and A. Van Der Schaft. The disturbance decoupling problem for nonlinear control systems. *IEEE Transactions on Automatic Control*, AC-28(5):621–623, 1983.

M. B. Estrada and M. Malabre. Necessary and sufficient conditions for disturbance decoupling with stability using PID control laws. *IEEE Transactions on Automatic Control*, 44(6):1311–1315, 2002.

Z. Gao. Active disturbance rejection control: A paradigm shift in feedback control system design. *Proceedings of the American Control Conference*, 14-16 June:2399–2405, 2006.

A. Nikoobin and H. N. Rahimi. Analyzing the wheeled mobile manipulators with considering the kinematics and dynamics of the wheels. *International Journal of Recent Trends in Engineering*, 1(5):90–92, 2009.

H. A. Zhu, C. L. Teo, G. S Hong, and A. N. Poo. Motion control of robotic manipulators with disturbance decoupling. *Second IEEE Control applications*, 1:397–402, 1993.

M. W. Chen and A. M. S. Zalzala. Dynamic modeling and genetic based trajectory generation for non-holonomic mobile manipulators. *Control Engineering Practice*, 5(1):39–48, 1997.

C. Wang and V. Kumar. Velocity control of mobile manipulators. *Proceedings IEEE Int. Robotics and Automation*, 2:713–718, 1993.

J. H. Chung and S. A. Velinsky. Modeling and control of a mobile manipulator. *Robotica*, 16:607–613, 1998.

Y. Yamamoto and X. Yun. Effect of the dynamic interaction on coordinated control of mobile manipulators. *IEEE Transactions on robotics and automation*, 12(5):816–824, 1996.

Y. Yamamoto and X. Yun. A modular approach to dynamic modeling of a class of mobile manipulators. *International Journal of Robotics and Automation*, 12(2):41–48, 1997.

Mohammad Danesh, Farid Sheikholeslam, and Mehdi Keshmiri. External force disturbance rejection in robotic arms: An adaptive approach. *IEICE Trans. Fundamentals*, E88-A(10):2504–2513, 2005.

Jagdish Joshi and Alan A. Desrochers. Modeling and control of a mobile robot subject to disturbances. *IEEE International Conference on Robotics and Automation*, 1:1508–1513, 1986.

Alberto Isidori. *Nonlinear Control Systems*. Springer, 2002.

T. Yoshikawa. *Foundations of Robotics: Analysis and control*. MIT Press, 1990.

Bill Goodwine and Jason Nightingale. The Effect of Dynamic Singularities on Robotic Control and Design. *Proceedings of the 2010 IEEE International Conference on Robotics and Automation*.

APPENDIX

Detailed expressions for all of the terms contained in the equations of motion for the system.

$$q_v = [^v q_1 \ ^v q_2 \ ^v q_3 \ ^v q_4]^T = [x_0 \ y_0 \ \theta_r \ \theta_l]^T$$

$$q_r = [^r q_1 \ ^r q_2]^T = [\theta_1 \ \theta_2]^T$$

$$M_r = \begin{bmatrix} \frac{1}{3}m_1 l_1{}^2 + \frac{4}{3}m_2 l_2{}^2 + m_2 l_2{}^2 \cos\theta_2 & \frac{1}{3}m_2 l_2{}^2 + m_2 l_2{}^2 \cos\theta_2 \\ \frac{1}{3}m_2 l_2{}^2 + \frac{1}{2}m_2 l_2{}^2 \cos\theta_2 & \frac{1}{3}l_2{}^2 m_2 \end{bmatrix},$$

$$C_{r1} = \begin{bmatrix} -\frac{1}{2}m_2 l_2{}^2 \dot\theta_2^2 \sin\theta_2 - m_2 l_2{}^2 \dot\theta_1^2 \dot\theta_2^2 \sin\theta_2 \\ \frac{1}{2}m_2 l_2{}^2 \dot\theta_1^2 \sin\theta_2 \end{bmatrix},$$

$$C_{r2}{}^{(i)} = 2 \sum_{j=1}^{m} \sum_{k=1}^{n} \sum_{h=max(i,k)}^{n} tr\left[\frac{\partial T_h}{\partial^r q_i} J_h \frac{\partial^2 T_h{}^T}{\partial^v q_j \partial^r q_k}\right] ^v \dot q_j \cdot ^r \dot q_k$$

$$+ \sum_{j=1}^{m} \sum_{k=1}^{n} \sum_{h=i}^{n} tr\left[\frac{\partial T_h}{\partial^r q_i} J_h \frac{\partial^2 T_h{}^T}{\partial^v q_j \partial^v q_k}\right] ^v \dot q_j \cdot ^v \dot q_k,$$

$$R_r{}^{(ij)} = \sum_{k=i}^{n} tr\left[\frac{\partial T_k}{\partial^r q_i} J_k \frac{\partial T_k{}^T}{\partial^v q_j}\right], \ 1 \le i \le n, \ 1 \le j \le m,$$

$$T_i = T_v A_1{}^0 A_2{}^1 \dots A_i{}^{i-1}, \ i = 1, \dots, n,$$

$$A_1{}^0 = \begin{bmatrix} \cos\theta_1 & -\sin\theta_1 & 0 & l_1 \cos\theta_1 \\ \sin\theta_1 & \cos\theta_1 & 0 & l_1 \sin\theta_1 \\ 0 & 0 & 1 & 0 \\ 0 & 0 & 0 & 1 \end{bmatrix},$$

$$J_v = \begin{bmatrix} \cos\phi & -\sin\phi \\ \sin\phi & \cos\phi \end{bmatrix}, J_{r1} = \begin{bmatrix} -(l_1/2)\sin\theta_1 & 0 \\ (l_1/2)\cos\theta_1 & 0 \end{bmatrix},$$

$$A_2{}^1 = \begin{bmatrix} \cos\theta_2 & -\sin\theta_2 & 0 & l_2 \cos\theta_2 \\ \sin\theta_2 & \cos\theta_2 & 0 & l_2 \sin\theta_2 \\ 0 & 0 & 1 & 0 \\ 0 & 0 & 0 & 1 \end{bmatrix},$$

$$T_v = \begin{bmatrix} \cos\phi & \sin\phi & 0 & x_0 \\ -\sin\phi & \cos\phi & 0 & y_0 \\ 0 & 0 & 1 & 0 \\ 0 & 0 & 0 & 1 \end{bmatrix},$$

$$J_{r2} = \begin{bmatrix} -l_1 \sin\theta_1 - (l_2/2)\sin(\theta_1+\theta_2) & -(l_2/2)\sin(\theta_1+\theta_2) \\ l_1 \cos\theta_1 + (l_2/2)\cos(\theta_1+\theta_2) & (l_2/2)\cos(\theta_1+\theta_2) \end{bmatrix}$$

$$M_{v2}{}^{(ij)} = \sum_{k=1}^{n} tr\left[\frac{\partial T_k}{\partial^v q_i} J_k \frac{\partial T_k{}^T}{\partial^v q_j}\right], \ 1 \le i, \ j \le m,$$

$$R_v{}^{(ij)} = \sum_{k=j}^{n} tr\left[\frac{\partial T_k}{\partial^v q_i} J_k \frac{\partial T_k{}^T}{\partial^r q_j}\right], \ 1 \le i \le m, \ 1 \le j \le n,$$

$$J_1 = \begin{bmatrix} \frac{1}{3}m_1 l_1{}^2 & 0 & 0 & -\frac{1}{2}m_1 l_1 \\ 0 & 0 & 0 & 0 \\ 0 & 0 & 0 & 0 \\ -\frac{1}{2}m_1 l_1 & 0 & 0 & m_1 \end{bmatrix},$$

$$J_2 = \begin{bmatrix} \frac{1}{3}m_2 l_2{}^2 & 0 & 0 & -\frac{1}{2}m_2 l_2 \\ 0 & 0 & 0 & 0 \\ 0 & 0 & 0 & 0 \\ -\frac{1}{2}m_2 l_2 & 0 & 0 & m_2 \end{bmatrix},$$

$$M_{v1} = \begin{bmatrix} m & 0 & -m_c cd \sin\phi & m_c cd \sin\phi \\ 0 & m & m_c cd \cos\phi & m_c cd \cos\phi \\ -m_c cd \sin\phi & m_c cd \cos\phi & Ic^2 + I_w & -Ic^2 \\ m_c cd \sin\phi & -m_c cd \cos\phi & -Ic^2 & Ic^2 + I_w \end{bmatrix},$$

$$C_{v1} = \begin{bmatrix} -m_c d\dot\phi^2 \cos\phi \\ -m_c d\dot\phi^2 \sin\phi \\ 0 \\ 0 \end{bmatrix}, E_v = \begin{bmatrix} 0 & 0 \\ 0 & 0 \\ 1 & 0 \\ 0 & 1 \end{bmatrix},$$

$$C_{v2}{}^{(i)} = 2 \sum_{j=1}^{n} \sum_{k=1}^{m} \sum_{h=j}^{n} tr\left[\frac{\partial T_h}{\partial^v q_i} J_h \frac{\partial^2 T_h{}^T}{\partial^r q_j \partial^v q_k}\right] ^r \dot q_j \cdot ^v \dot q_k$$

$$+ \sum_{j=1}^{n} \sum_{k=1}^{n} \sum_{h=max(j,k)}^{n} tr\left[\frac{\partial T_h}{\partial^v q_i} J_h \frac{\partial^2 T_h{}^T}{\partial^r q_j \partial^r q_k}\right] ^r \dot q_j \cdot ^r \dot q_k,$$

$$\Phi = \begin{bmatrix} \Phi_{1,1} & \Phi_{1,2} & 0 & 0 \\ \Phi_{2,1} & \Phi_{2,2} & 0 & 0 \\ 0 & 0 & \Phi_{3,3} & \Phi_{3,4} \\ 0 & 0 & \Phi_{4,3} & \Phi_{4,4} \end{bmatrix},$$

$\Phi_{1,1} = (cb - l_y c)\cos\phi - l_x \sin\phi$, $\Phi_{1,2} = (cb + l_y c)\cos\phi + l_x \sin\phi$,

$\Phi_{2,1} = (cb - l_y c)\sin\phi + l_x \cos\phi$, $\Phi_{2,2} = (cb + l_y c)\sin\phi - l_x \cos\phi$,

$\Phi_{3,3} = -l_1 \sin\theta_1 - l_2 \sin(\theta_1 + \theta_2)$, $\Phi_{3,4} = -l_2 \sin(\theta_1 + \theta_2)$,

$\Phi_{4,3} = l_1 \cos\theta_1 + l_2 \cos(\theta_1 + \theta_2)$, $\Phi_{4,4} = l_2 \cos(\theta_1 + \theta_2)$.